Supplementary figures

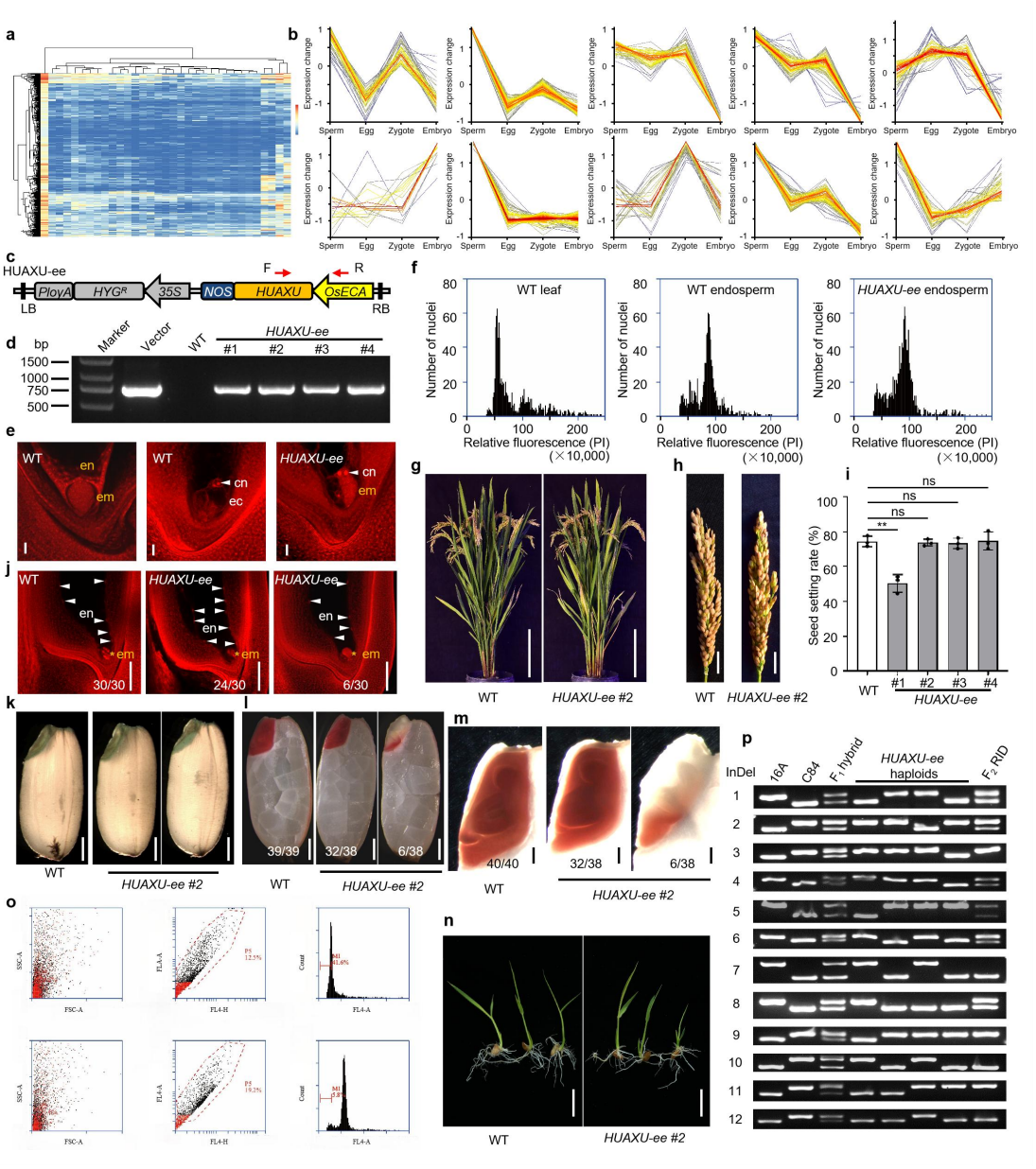

Supplementary Fig. S1 Ectopic expression of *HUAXU* in egg cells, related to Fig. 1

a Heatmap of expression levels for 729 sperm-specific genes across diverse tissues and cell types. Color scale indicates $\log_2$(TPM+1), with highest expression in sperm cells (first column). **b** Time-series clustering of sperm-specific genes in sperm cells, egg cells, zygotes, and embryos. **c** Schematic of primer positions for PCR detection of the HUAXU-ee cassette. **d** PCR confirmation of HUAXU-ee cassette integration in independent T_0 transgenic lines. Binary vector, positive control; WT (CY84) genomic DNA, negative control. **e** Eosin B-stained ovaries showing absence of autonomous endosperm development in *HUAXU-ee* lines. WT ovaries at 2 days after flowering (DAF) (left; pollinated), WT (middle) and *HUAXU-ee* (right) ovaries at 3 days after emasculation. Pollinated WT ovaries contain well-developed endosperm (en), whereas unfertilized ovaries of both genotypes lack endosperm and retain only unfused central cell nuclei (cn, arrowheads). *n* > 30. ec, egg cell; em, embryo. Scale bars, 20 μm. **f**

Flow-cytometric ploidy analysis of endosperm in *HUAXU-ee* lines. Histograms of propidium iodide (PI)-stained nuclei from WT leaf, WT endosperm, and *HUAXU-ee* endosperm. *HUAXU-ee* endosperm shows triploid DNA content, consistent with fertilization-dependent development. **g**, **h** Morphology of *HUAXU-ee* T_0 plants. Representative whole-plant (**g**) and panicle (**h**) images of WT and *HUAXU-ee* T_0 plants. Scale bars, 20 cm (**g**) and 2 cm (**h**). **i** Seed-setting rate in *HUAXU-ee* T_0 lines vs WT. ***P* < 0.01; ns, *P* ≥ 0.05 (two-tailed Student's *t*-test). **j** Precocious embryo development in *HUAXU-ee* ovules triggered by ectopic *HUAXU* expression. Eosin B-stained ovules at 1 DAF from WT (left) and *HUAXU-ee* lines (middle, right). Endosperm development is comparable between genotypes, but precocious embryos (orange asterisks) appear in a subset of *HUAXU-ee* ovules. White arrowheads mark free endosperm nuclei. em, embryo; en, endosperm. Scale bars, 100 μm. **k**–**m** Mature seeds (**k**), TTC-stained mature seeds (**l**), and magnified embryos (**m**) from WT and *HUAXU-ee* lines (*n* > 30). Scale bars, 0.1 mm (**k** and **l**) and 0.02 mm (**m**). **n** 5-day-old seedlings from WT and *HUAXU-ee* seeds. Scale bars, 2 cm. **o** Gating strategy for flow-cytometric identification of haploids. Representative profiles for haploid (top) and diploid (bottom) nuclei; identical gating applied across all samples. **p** Genotyping of *HUAXU-ee* derived haploids using InDel markers. Cropped gel images of 12 chromosome-specific InDel markers in *HUAXU-ee* haploids and diploid recombinant inbred plants (RID). Haploids confirmed by single-band patterns across all markers. 16A and C84 are the parental lines of F_1 hybrid CY84 (WT).

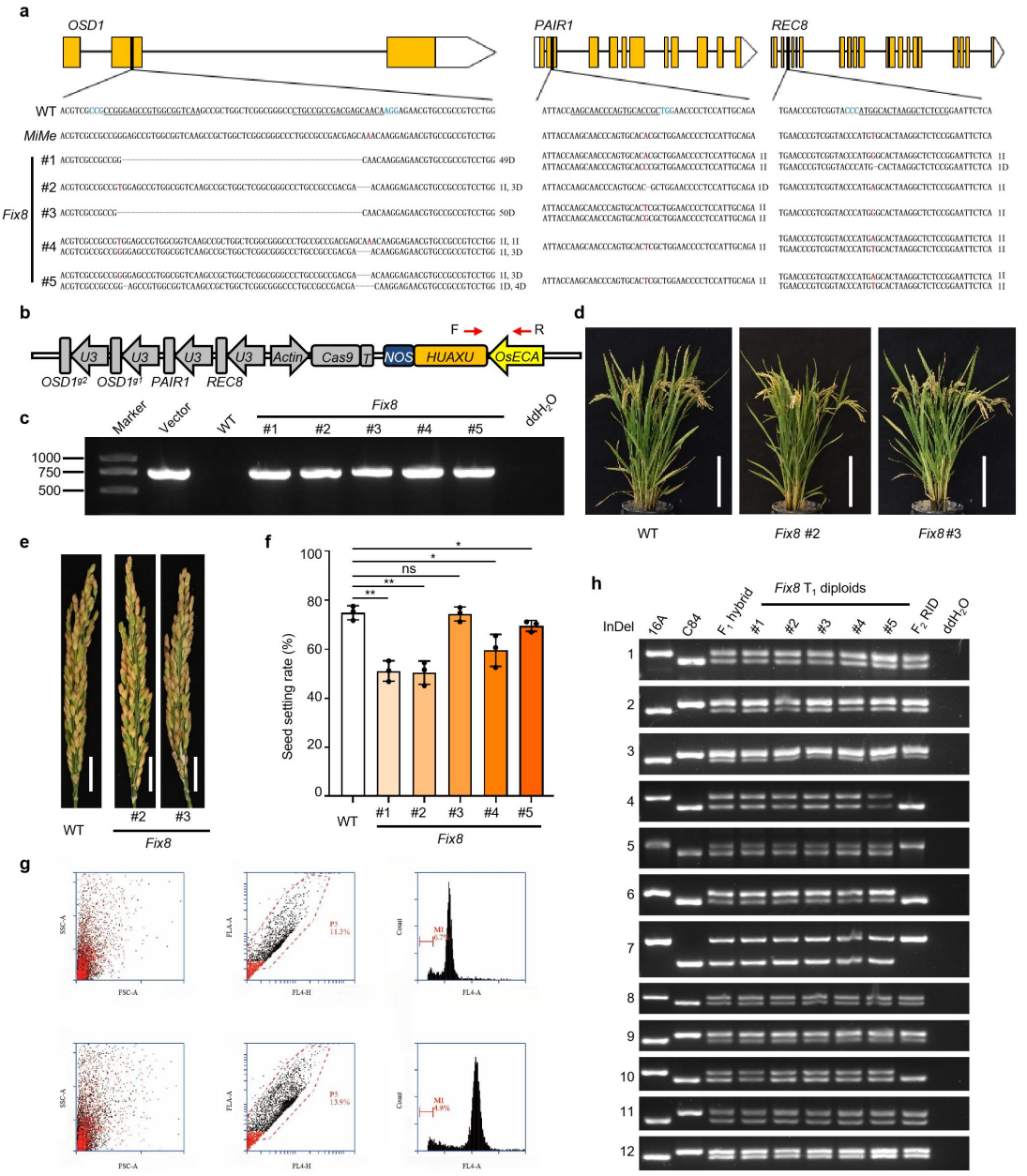

Supplementary Fig. S2 Generation and verification of the *Fix8* apomictic hybrid rice, related to Fig. 2

a Genotyping of *OSD1*, *PAIR1*, and *REC8* mutations in *MiMe* and *Fix8* T_0 plants by Hi-TOM sequencing. PAM sites are highlighted in blue, sgRNA target sequences are underlined, inserted bases are shown in red, and deleted bases are indicated by red dotted lines. **b**, **c** PCR detection of the egg cell-specific HUAXU-ee expression cassette in *Fix8* T_0 lines. Red arrows mark primer binding sites (**b**). The binary vector served as a positive control; genomic DNA from WT plants and ddH_2O were negative controls (**c**). **d**, **e** Representative plant (**d**) and panicle (**e**) morphology of WT and *Fix8* T_0 plants. Scale bars, 20 cm (**d**) and 2 cm (**e**). **f** Seed-setting rate of *Fix8* T_0 plants compared to WT. Data are mean ± SD from three primary panicles per plant. $^{**}P < 0.01$; $^{*}P < 0.05$; ns, not significant ($P \geq 0.05$; two-tailed Student's *t*-test). **g** Flow cytometry gating strategy for ploidy analysis of diploid and tetraploid samples. A

consistent gating strategy was applied to all samples. Representative profiles are shown for diploids (top) and tetraploids (bottom). **h** InDel marker genotyping of diploid progeny from *Fix8* T_0 lines. Cropped gel images display genotypes across 12 chromosome-specific InDel markers for diploid progeny derived from *Fix8* T_0 plants and F_2 recombinant inbred diploids (RID) from the F_1 hybrid CY84. All *Fix8*-derived diploids retain heterozygosity at every marker, identical to the F_1 hybrid CY84 (WT), confirming clonal propagation. 16A and C84 denote the two parental lines of CY84.

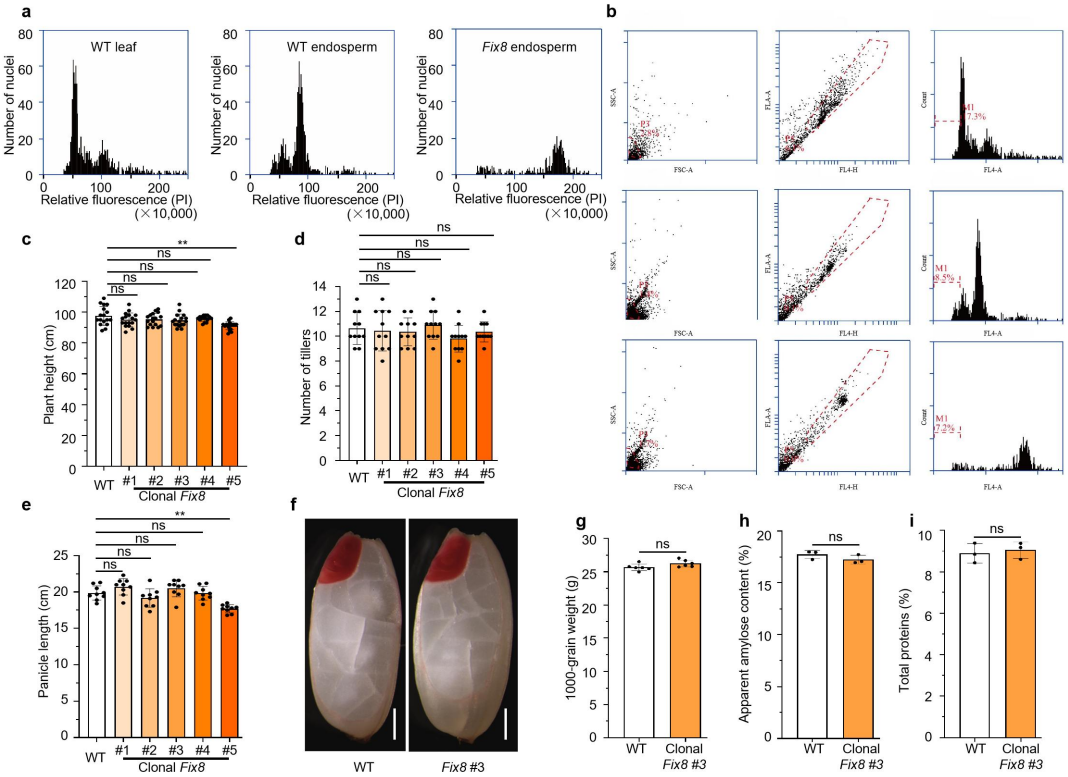

Supplementary Fig. S3 Plant and mature seed phenotypes of clonal *Fix8*, related to Fig. 3

a Flow cytometric ploidy analysis of clonal *Fix8* endosperm. Histograms of propidium iodide (PI)-stained nuclei from WT (CY84) leaf (diploid reference), WT endosperm (triploid reference), and *Fix8* endosperm. *Fix8* endosperm shows hexaploid DNA content, consistent with fertilization-dependent development. **b** Standardized gating strategy for endosperm ploidy analysis by flow cytometry. Representative histograms display dominant peaks for diploid (top), triploid (middle), and hexaploid (bottom) nuclei. **c**–**e** Phenotypes of clonal *Fix8* in the T_1 generation. Plant height (**c**), tiller number (**d**), and panicle length (**e**) in WT and clonal *Fix8*. Data are mean ± SD from independent plants. $^{**}P < 0.01$; ns, not significant ($P \geq 0.05$; two-tailed Student's *t*-test). **f** Embryo viability in mature clonal *Fix8* seeds assessed by TTC staining. Comparable red deposition in embryos from WT and clonal *Fix8* seeds ($n > 30$), indicating unimpaired viability. Scale bars, 0.1 mm. **g**–**i** Yield and nutritional phenotypes of clonal *Fix8* seeds. 1000-grain weight (**g**), apparent amylose content (**h**), and total protein content (**i**) in WT and clonal *Fix8* #3 seeds. Data are mean ± SD from independent plants. ns, not significant ($P \geq 0.05$; two-tailed Student's *t*-test).

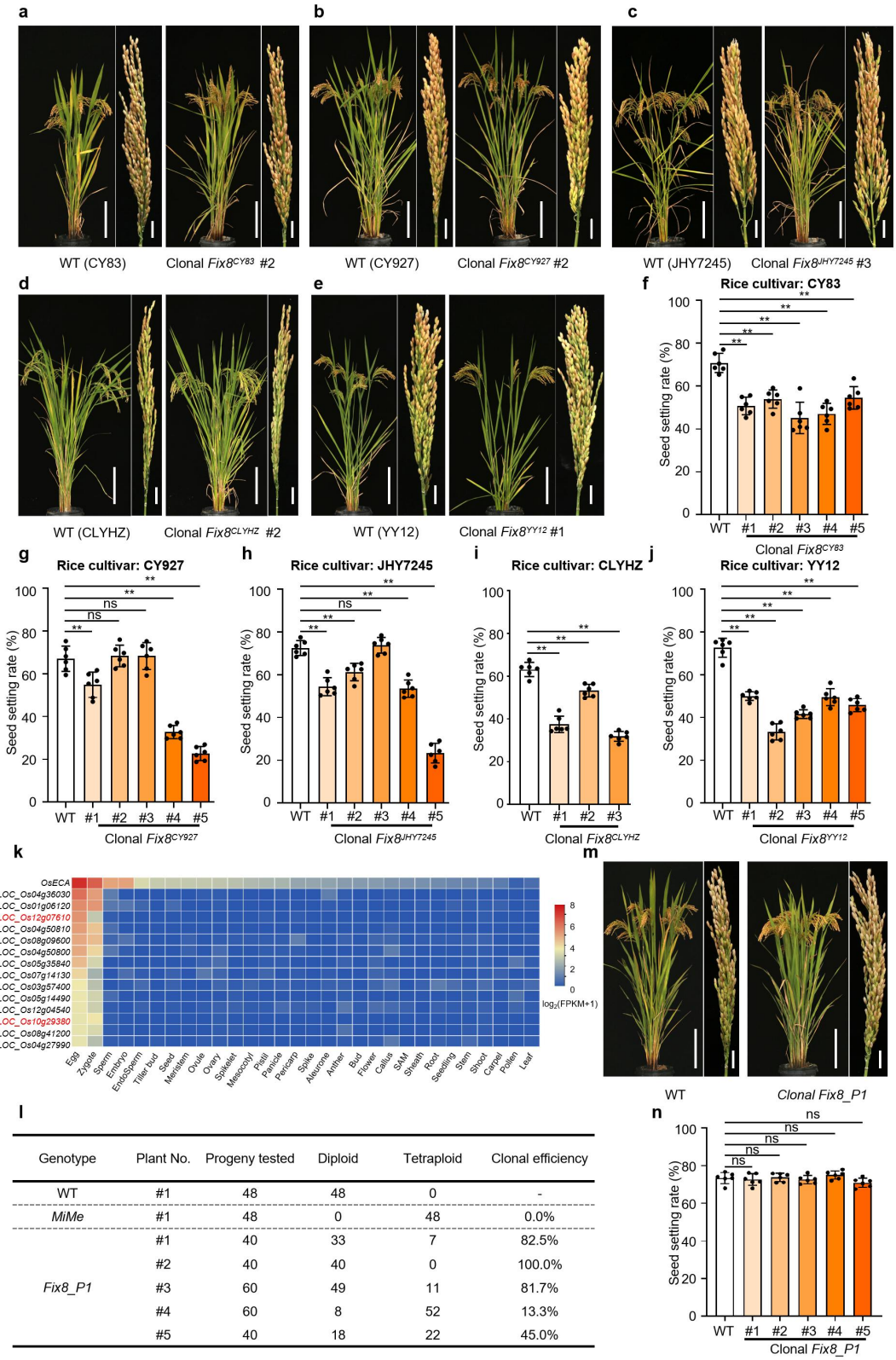

l

Genotype	Plant No.	Progeny tested	Diploid	Tetraploid	Clonal efficiency
WT	#1	48	48	0	-
MiMe	#1	48	0	48	0.0%
Fix8_P1	#1	40	33	7	82.5%
	#2	40	40	0	100.0%
	#3	60	49	11	81.7%
	#4	60	8	52	13.3%
	#5	40	18	22	45.0%

Supplementary Fig. S4 Variety testing and fertility optimization of the *HUAXU*-based apomictic system, related to Fig. 4

a–**e** Representative plant and panicle morphology of clonal *Fix8* T_1 progeny and corresponding wild-type (WT) plants in multiple hybrid rice cultivars: Chunyou83 (CY83; **a**), Chunyou927

(CY927; **b**), Jiaheyou7245 (JHY7245; **c**), CLiangyouhuazhan (CLYHZ; **d**), and Yongyou12 (YY12; **e**). Scale bars, 20 cm (plants) and 2 cm (panicles). **f**–**j** Seed setting rates of clonal *Fix8* T_1 progeny compared to WT across the hybrid rice cultivars shown in (**a**–**e**). Data are mean ± SD from randomly selected independent plants. $^{**}P < 0.01$; ns, not significant ($P \geq 0.05$; two-tailed Student's *t*-test). **k** Heatmap of expression profiles for 14 egg cell–specific candidate genes across diverse rice tissues and cell types. Genes were selected for undetectable expression (FPKM < 1.0) in all non–egg and non-zygote cells. The color scale represents $\log_2$(FPKM+1) values. *OsECA*, a known egg cell–specific marker gene, is included as reference. **l** Ploidy analysis of progeny derived from wild-type (WT; CY83), *MiMe* (CY83), and *Fix8_P1* lines. Ploidy levels were determined by flow cytometry combined with field-based phenotypic evaluation. **m** Representative plant and panicle morphology of WT (CY83) and clonal *Fix8_P1* progeny grown under paddy field conditions. Scale bars, 20 cm (plants) and 2 cm (panicles). **n** Seed setting rate of clonal *Fix8_P1* T_1 plants vs WT (CY83). Data are mean ± SD (n = 6 plants, 3 primary panicles per plant). $^{**}P < 0.01$; ns, not significant ($P \geq 0.05$; two-tailed Student's *t*-test).

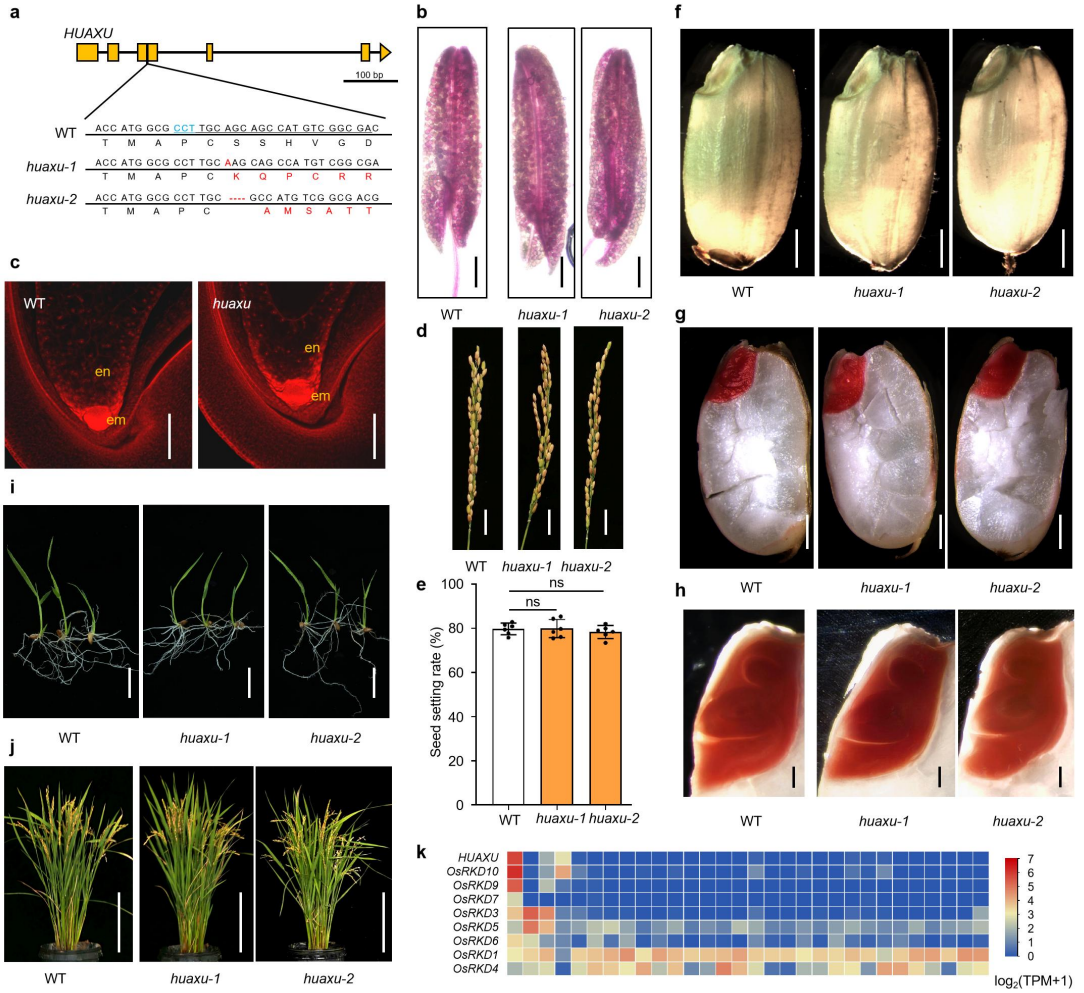

Supplementary Fig. S5 Phenotypic analysis of *huaxu* mutants

a Genotypes of *huaxu* mutants generated by CRISPR/Cas9 genome editing. Mutant alleles are shown with the PAM site highlighted in blue, inserted nucleotides in red, and deleted nucleotides indicated by red dashes. **b** Loss of *HUAXU* does not affect pollen fertility. Alexander staining of mature anthers from wild-type (WT; NIP) and *huaxu* mutants (n > 30). Scale bars, 200 μm. **c** Loss of *HUAXU* does not disrupt early embryo development. Eosin B-stained developing seeds at 4 DAF from WT (NIP; left) and *huaxu* mutants (right) (n > 30). em, embryo; en, endosperm. Scale bars, 100 μm. **d** Panicle morphology of WT (NIP) and *huaxu* mutants. Scale bars, 2 cm. **e** Seed-setting rate of *huaxu* mutant plants relative to WT (NIP). Data are mean ± SD from six plants (three primary panicles per plant). ns, not significant (P ≥ 0.05; two-tailed Student's t-test). **f**–**h** Loss of *HUAXU* does not impair mature embryo viability. Mature seeds (**f**), TTC-stained mature seeds (**g**), and enlarged views of TTC-stained embryos (**h**) from WT (NIP) and *huaxu* mutants. Scale bars, 0.1 mm (**f** and **g**) and 0.02 mm (**h**). **i**, **j** Loss of *HUAXU* does not affect rice vegetative growth. Representative phenotypes of young seedlings at 5 DAG (**i**) and mature plants (**j**) from WT (NIP) and *huaxu* mutants. Scale bars, 2 cm (**i**) and 20 cm (**j**). **k** Heatmap of expression levels of the nine rice RKD genes across tissues and cell types. Four genes, including *HUAXU*, *OsRKD7*, *OsRKD9*, and *OsRKD10*,

show sperm cell-specific expression. Color scale represents $\log_2$(TPM+1) values; the first and second columns correspond to sperm cells and egg cells, respectively.

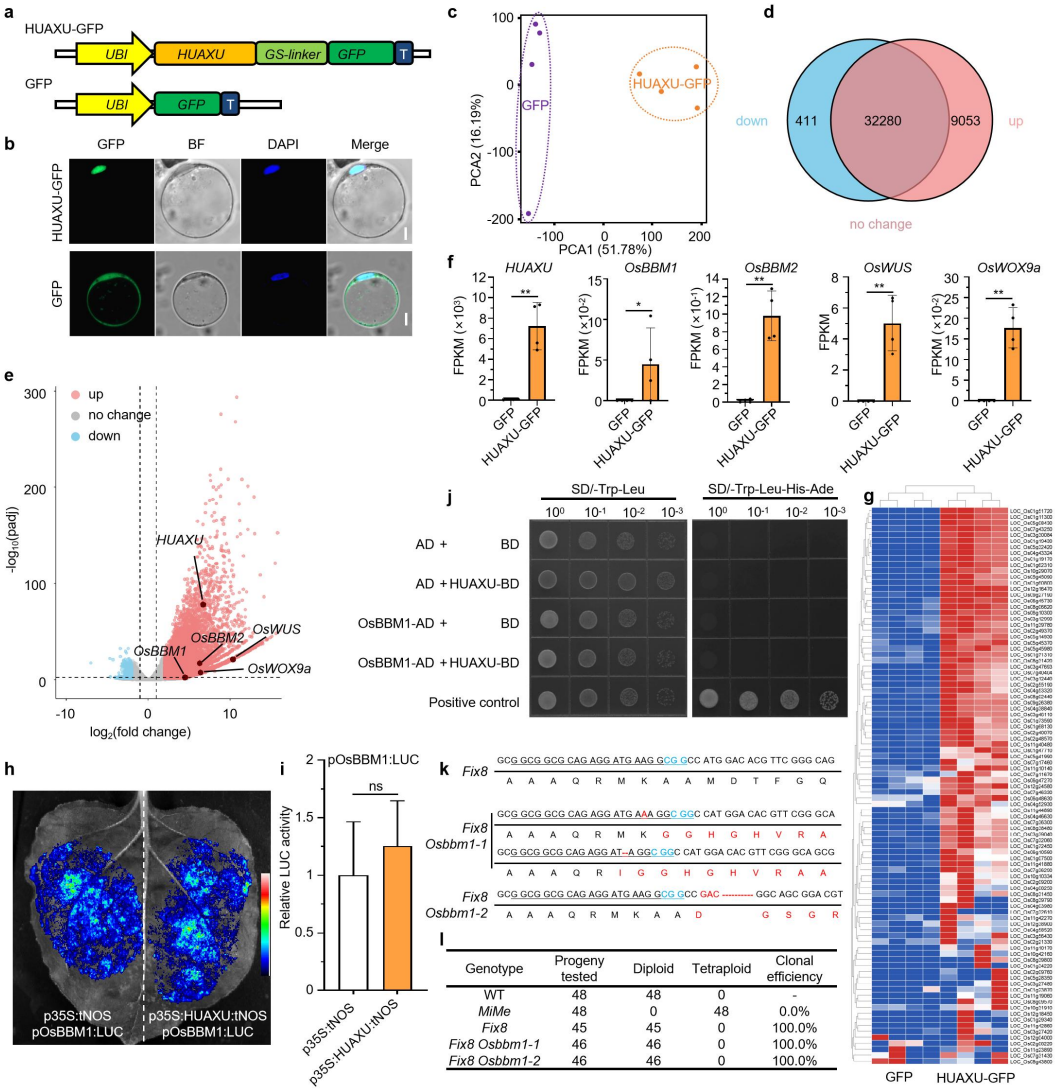

Supplementary Fig. S6 *HUAXU* likely drives parthenogenesis independently of *OsBBM1*

a Schematic of the UBI:HUAXU-GFP construct and free GFP control vector. **b** Transient expression of HUAXU-GFP or free GFP in rice protoplasts. Nuclei were counterstained with DAPI (blue). HUAXU-GFP localizes to the nucleus and co-localizes with DAPI; free GFP is distributed throughout the cell. Scale bars, 5 μm. **c** Principal component analysis (PCA) of RNA-seq profiles from rice protoplasts 16 h after transformation with UBI:HUAXU-GFP or UBI:GFP constructs. **d** Venn diagram showing the number of differentially expressed genes (DEGs; $|\log_2\text{fold change}| \geq 2$, adjusted $P < 0.05$) in HUAXU-GFP expressing protoplasts vs GFP controls. **e** Volcano plot of DEGs. Known parthenogenesis-associated genes that are up-regulated are labeled. **f** FPKM values of selected up-regulated parthenogenesis-associated genes in HUAXU-GFP vs GFP samples. $^{**}P < 0.01$; $^{*}P < 0.05$; (Benjamini–Hochberg adjusted P values for multiple testing). **g** HUAXU activates egg-to-zygote *de novo* expressed genes. Of 164 such genes detected, 93 were activated or up-regulated in HUAXU-GFP protoplasts. Color scale represents FPKM values, with each row normalized per gene. **h**, **i** Luminescence imaging (**h**) and quantification of luciferase (LUC) activity (**i**) in transient dual-luciferase

reporter assays in *Nicotiana benthamiana* leaves. Effector and reporter constructs were co-infiltrated as indicated; an empty p35S::tNOS vector served as negative control. Assays were performed in three independent experiments, with ≥3 leaves infiltrated and imaged per combination in each experiment. ns, not significant ($P \geq 0.05$; two-tailed Student's *t*-test). **j** Yeast two-hybrid assay showing no interaction between HUAXU and OsBBM1. HUAXU was fused to the GAL4 DNA-binding domain (BD) and tested against OsBBM1 fused to the activation domain (AD). Empty AD and BD vectors served as negative controls; D53-AD and IPA1-BD served as positive controls. Representative plates from three independent experiments are shown. **k** CRISPR/Cas9-mediated knockout of *OsBBM1* in *Fix8* line #3 (carrying the sgMiMe_HUAXU-ee construct). The PAM site is highlighted in blue, inserted nucleotides in red, and deleted nucleotides indicated by red dashes. **l** Diploid progeny ratio in selfed progeny of the indicated genotypes, determined by flow cytometry analysis of nuclear DNA content.

Supplementary Tables

Supplementary Tables S1, S2, S5, S7, S9, and S10 are provided as separate Excel files. The remaining supplementary tables are presented as follows:

Supplementary Table S3 Primers for Insertion-deletion (InDel) markers between 16A and C84 used in this study

Name	Chr	Primer forward (5′–3′)	Primer reverse (5′–3′)
InDel01	1	GTTATTTCACCCGGGTCTTTAGTC	CTCTAACCGTGTCATTCTTACTCAGG
InDel02	2	CGTGGCCATCTTGTAGTGG	GTAGACAGAGATGGGGTAGACG
InDel03	3	CTTGCCCATCAGCCTATCAC	ACACGTACACAGCCATGAGA
InDel04	4	TGCCTCTTTCGAACGTATCC	TAAGCTACGAGCAGTGGACAC
InDel05	5	TCAGTACAAGGCACCCATGC	GAGGGAGTACCAACTTGCTG
InDel06	6	GGTCCTCCATCGAGCAGTATC	GCCTAGCAAGACATGGACCTC
InDel07	7	GCACAAAGGTAGCGTGAGAC	GAAGGTTTTCTATACACTATAACTGCCTTG
InDel08	8	AGGTCTTCTGTCCAAGTTCATTG	AACCATATAAACTCATCTGCACAACTC
InDel09	9	CTACAATCGCATTCTTGTGAGGAC	AGAGGCGGTTACCATCTGC
InDel10	10	CTTCAAGTGAGGTCCTTCACTATG	ATATGTGGCGGTATGGCTTTC
InDel11	11	CGTGGGCATCATTAAGGCTTG	TGCCTGGCGATCTCTGTGAG
InDel12	12	GTGGAGCTCTCTCACGAAATG	CTATTGGAGAGATAAGGATTTCTTATGCAG

146 **Supplementary Table S4 Hybrid rice cultivars used in this study**

147

Full name	Short name	Male sterile line (♀)	Restorer line (♂)
Chunyou 84	CY84	Chunjiang 16A	C84
Chunyou 83	CY83	Chunjiang 88A	T27
Chunyou 927	CY927	Chunjiang 16A	C927
Jiaheyou 7245	JHY7245	Jiahe 212A	Zhonghui 7245
Cliangyou Huazhan	CLYHZ	C815S	Huazhan
Yongyou 12	YY12	Yonggeng 2A	F5032

Table S6 Ploidy analysis of the progeny from WT and *Fix8* T_0 lines in different cultivars

Genotype	Plant No.	Progeny tested	Diploid	Tetraploid	Clonal efficiency
WT (CY84)	#1	48	48	0	-
MiMe^{CY84}	#1	48	0	48	0.0%
Fix8^{CY83}	#1	64	64	0	100.0%
	#2	48	48	0	100.0%
	#3	32	32	0	100.0%
	#4	48	48	0	100.0%
	#5	48	48	0	100.0%
Fix8^{CY927}	#1	48	48	0	100.0%
	#2	48	48	0	100.0%
	#3	40	40	0	100.0%
	#4	56	56	0	100.0%
	#5	32	32	0	100.0%
Fix8^{JHY7245}	#1	48	48	0	100.0%
	#2	48	48	0	100.0%
	#3	48	48	0	100.0%
	#4	40	40	0	100.0%
	#5	32	32	0	100.0%
Fix8^{CLYHZ}	#1	48	48	0	100.0%
	#2	48	48	0	100.0%
	#3	32	32	0	100.0%
Fix8^{YY12}	#1	32	32	0	100.0%
	#2	32	32	0	100.0%
	#3	32	32	0	100.0%
	#4	48	48	0	100.0%
	#5	48	48	0	100.0%

Table S8 FPKM expression values of RNA-seq from WT and *HUAXU-ee* ovaries 2 days after emasculation

Genes	WT-1	WT-2	WT-3	*HUAXU-ee*-1	*HUAXU-ee*-2	*HUAXU-ee*-3
HUAXU	0	0	0	0.274176	0	0
OsBBM1	0	0	0	0.324504	0.15062	0.01344
OsBBM2	0	0	0	0	0.013772	0
OsWUS	0	0	0	0.059914	0	0
OsWOX9a	0.702419	0.522516	0.51573	0.349228	0.866828	1.492182